

SEP 22 1987

CONF-8708143--2

Los Alamos National Laboratory is operated by the University of California for the United States Department of Energy under contract W-7405-ENG-36

TITLE: RESULTS OF RECENT CALCULATIONS USING REALISTIC POTENTIALS

LA-UR--87-2797

DE87 014769

AUTHOR(S): J. L. Friar, T-5

SUBMITTED TO: Invited lecture at "XIth European Conference
on Few-Body Physics", Fontevraud, France,
August 31 - September 5, 1987.**DISCLAIMER**

This report was prepared as an account of work sponsored by an agency of the United States Government. Neither the United States Government nor any agency thereof, nor any of their employees, makes any warranty, express or implied, or assumes any legal liability or responsibility for the accuracy, completeness, or usefulness of any information, apparatus, product, or process disclosed or represents that its use would not infringe privately owned rights. Reference herein to any specific commercial product, process, or service by trade name, trademark, manufacturer, or otherwise does not necessarily constitute or imply its endorsement, recommendation, or favoring by the United States Government or any agency thereof. The views and opinions of authors expressed herein do not necessarily state or reflect those of the United States Government or any agency thereof.

By acceptance of this article, the publisher recognizes that the U.S. Government retains a nonexclusive, royalty-free license to publish or reproduce the published form of this contribution, or to allow others to do so, for U.S. Government purposes.

The Los Alamos National Laboratory requests that the publisher identify this article as work performed under the auspices of the U.S. Department of Energy.

Los Alamos Los Alamos National Laboratory
Los Alamos, New Mexico 87545

MASTER

JMF

RESULTS OF RECENT CALCULATIONS USING REALISTIC POTENTIALS

J. L. Friar
Theoretical Division, Los Alamos National Laboratory
Los Alamos, NM 87545 USA

Abstract

Results of recent calculations for the triton using realistic potentials with strong tensor forces are reviewed, with an emphasis on progress made using the many different calculational schemes. Several test problems are suggested.

Introduction

Many different calculational techniques have been used to solve the Schrödinger equation for the triton. The most common [1-4] of these techniques historically, and the oldest, is the Raleigh-Ritz variational procedure. This august method predates quantum mechanics, and still provides an effective procedure for solving the Schrödinger equation for the few-nucleon problem. In order to implement this scheme one only needs to construct a trial wavefunction, ψ_T , and form $E_u = \langle \psi_T | H | \psi_T \rangle$, where H is the Hamiltonian in question. The quantity E_u is an upper bound for the exact energy, E : $E_u \geq E$. If the difference of the trial wave function from the exact wave function, ψ , can be characterized by a (small) parameter ϵ [$\psi_T = \psi + \text{order}(\epsilon)$] then $E_u = E + \text{order}(\epsilon^2)$. Lower bounds for the eigenvalue, E , can also be constructed [5], whose quality is significantly lower: $E_l = E + \text{order}(\epsilon)$.

The Green's function Monte Carlo (GFMC) method is the oldest [6] method used to solve the Schrödinger equation "exactly" for local potentials (square, exponential, and gaussian). It is also probably the least well-known [4,7] in our community. The two primary ingredients are the use of imaginary time ($t \rightarrow -i\tau$) for the bound-state Schrödinger equation, which renders the exponential time dependence real, and representing the wavefunction by a set of points (or delta functions) in the nuclear Hilbert

space. The points are randomly selected. The beauty of this procedure is that if the points can be chosen in a physically reasonably way, relatively few of them are needed, even to represent a function in a multidimensional Hilbert space. The time-dependent Schrödinger equation is solved by iteration, each iteration advancing the (imaginary) time by an amount $\Delta\tau$. In common with most iterative methods, this technique will converge to the lowest eigenstate of the Hamiltonian. This can be seen if we represent the Schrödinger equation solution by a spectral expansion and take the large τ limit: $\exp((E_0 - H)\tau)\psi = \sum_n \exp(-(E_n - E_0)\tau)a_n\phi_n \rightarrow a_0\phi_0$, where the ϕ_n are the eigenstates of H with eigenvalues, E_n , of which E_0 is the lowest. The initial distribution ψ can be any admixture of the ϕ_n 's, but clearly one's final accuracy depends on the size of a_0 in the initial distribution. In addition, a relatively large quadrature error associated with Monte Carlo methods is unavoidable.

The hyperspherical harmonic (HH) expansion technique was popularized in nuclear physics by Simonov and collaborators [8]. It is used in atomic physics and has been extensively applied in recent years to both the triton and alpha particle by the Orsay [9] and Kurchatov [10] groups. Unlike many (but not all) of the variational approaches, this technique is constructive. That is, the expansion of the wavefunction is made in terms of a complete set, and adding more terms should improve the quality of the expansion. Convergence then requires only that enough terms are used, or that the important ones can be chosen from the complete set.

The fourth technique which is used is the Faddeev approach [11-13]. The seminal work of Faddeev in formulating a scheme for implementing the boundary conditions for the scattering of three particles is also an exceptionally useful (and tractable) technique for solving bound state problems [14], whether in momentum space, configuration space, or a mixture of the two. The original solution for a subset of partial waves of a "realistic" local potential was achieved by Malfliet and Tjon [15]. Since that time the Faddeev method has proven to be the most accurate method for the triton, if not the easiest to implement.

Results for Test Potentials

Much of the testing for these computational methods has involved simple test potentials, most of which are unphysical. In addition, many of the groups performing these calculations have favorite potentials which are not used by the others. Consequently it has proven very difficult to make comparisons. The one exception is the spin- and isospin-independent Malfliet-Tjon V (MTV) potential [5,15]. The triton binding energies, E_B ,

Table 1. MTV triton binding energies in MeV.

	<u>UA[19]</u>	<u>Rome[3]</u>	<u>Sapporo[1]</u>	<u>Orsay[17]</u>	<u>GPMC[18]</u>	<u>LAFG[5]</u>
E_B :	8.22(2)	8.244	8.26	8.251	8.26(1)	8.251

(in MeV) obtained for this potential by various groups are given in table 1. The first three methods are variational upper bounds, the next two are a recent hyperspherical result and the GPMC solution, while the last one is a Los Alamos (-Iowa) Faddeev Group (LAFG) result. Using the wavefunctions obtained by solving the Faddeev equations, the latter group obtained a variational upper bound of $E_u = -8.253$ MeV and a lower bound of -8.484 MeV, while the Sapporo group found a lower bound of -8.9 MeV. The agreement between all of these calculations is excellent.

Results for Realistic Potentials

Variational results have been obtained for a variety of potentials with strong tensor forces. Unfortunately, common potentials are rarely used by two or more groups. The Sapporo [1] and Urbana-Argonne (UA) groups [19,20] have calculated with the Reid Soft Core V_8 model. This model uses the 1S_0 RSC potential in all singlet-even waves, the 1P_1 potential in all singlet-odd waves, the 3S_1 - 3D_1 potential in all triplet-even waves, and the 3P_2 - 3F_2 potential in all triplet-odd waves. It is constructed so that there are no \vec{L}^2 or $(\vec{L} \cdot \vec{S})^2$ components; it has only central, tensor, and spin-orbit components and is local. The UA results are $E_u = -6.86(8)$ MeV [16] or $-6.92(9)$ MeV [20] while the Sapporo group finds -7.13 MeV. Recently at Los Alamos we have solved the 34-channel problem with this potential, which utilizes all nucleon-nucleon partial waves with total angular momentum $J \leq 4$. We find $E = -7.56$ MeV, which is substantially lower than both variational results. The V_8 potentials are so constructed that they are identical in the 1S_0 , 3S_1 - 3D_1 partial waves which comprise the Faddeev 5-channel potential approximation. The Sapporo group's result for the latter potential is in excellent agreement with the consensus of Faddeev 5-channel calculations. Thus, the origin of the large disagreement is something of a mystery. We also note that the difference of .54 MeV between the 5-channel (positive parity, $J \leq 1$ NN partial waves) and 34-channel calculations is much larger than usual. The UA group [20] have also calculated with the AV14 potential and find $E = -7.16(2)$ MeV compared to a 34-channel result of -7.68 MeV.

Hyperspherical harmonic methods have been applied to the softer realistic potentials by the Orsay group [21]. They find -7.13 MeV for the Super Soft Core (C) potential, for which 34-channel Faddeev comparison results [14] exist: -7.53 MeV. Recently the Kurchatov group [22] have

indicated that they have greatly improved the convergence of their HH results, but no written discussion of these calculations has been available. This would be very exciting news.

Significant recent progress [7,23] has been made in utilizing the GFMC method to solve both the triton and alpha particle problems with realistic potentials. It is typical of applications of the Monte Carlo method to quantum mechanical problems that they have severe problems treating fermions [24]. In the most naive sense the Monte Carlo techniques require a positive (semi-) definite probability distribution from which to sample. The ground-state wave function for boson systems has such a distribution, in order to avoid nodal surfaces which increase the kinetic energy. In contradistinction, fermion ground states must have such surfaces in order to satisfy the Pauli principle. This is less true in few-nucleon systems because the angular momentum barrier renders the s-waves and the concomitant tensor-coupled d-waves dominant. Moreover, in the absence of spin- and isospin-dependent forces a completely space-symmetric solution for the triton and alpha particle results, which also satisfies the constraints of the Pauli principle. The net result is that the physical few-nucleon ground states are predominantly space-symmetric S-states, with admixtures of mixed symmetry S-, P-, and D-waves. The latter are not positive definite, but are not dominant.

Until recently, the GFMC method was believed not to work well for realistic potentials in the triton and alpha particle. The reason is that, in general, the ground state of the many-fermion Hamiltonian is not the solution which satisfies the Pauli principle and is antisymmetric, but rather a symmetric one which has no nodal planes that greatly enhance the kinetic energy. Convergence would then tend toward an unphysical state. It is part of the GFMC methodology to project such solutions out of the (random) distribution of points which represents the wave function. However, although they can be eliminated "in the mean", their effect on the Monte Carlo variance can not be eliminated and this "noise" eventually dominates and swamps the signal.

Joe Carlson, a member of our group, has recently succeeded [7] in applying the GFMC method to the triton and alpha particles for a quasi-realistic potential which has a strong tensor force. The potential used was the Argonne V_6 (AV6), and was chosen for the technical reason that it has no spin-orbit interaction (one simply eliminates the 7-14 components of the AV14 potential [25]). Converged answers were obtained without excessive noise. The triton energy result agrees with the Faddeev calculations: -7.148 MeV. The alpha particle results are shown in Figure 1, which is typical of the output of the GFMC procedure. The first

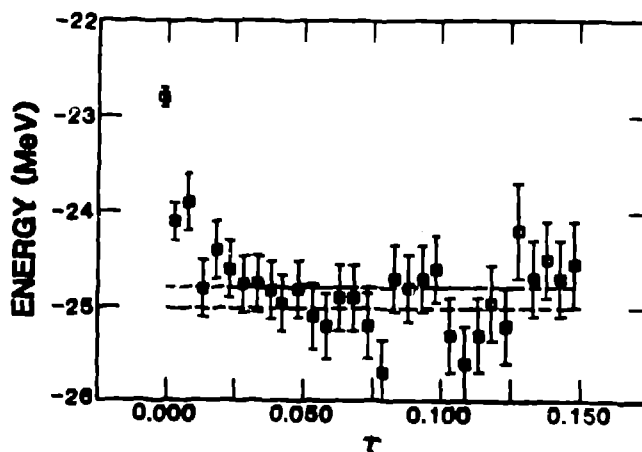


Figure 1. "Time dependence" of the GFMC alpha particle binding energy.

point at $\tau=0$ is the variational result and the source of the starting distribution for the GFMC procedure. As τ increases, the energy rapidly drops to a flat distribution modulated by random (statistical) errors. The dashed lines indicate $\pm\sigma$ for the final (constant) distribution. The time constant is less than $0.025 = 1/(40 \text{ MeV})$ which indicates that in the initial sample there are very energetic components, ϕ_n , which rapidly decay. Convergence is somewhat less rapid for the more weakly bound triton. The (preliminary) result of $E = -24.9(2) \text{ MeV}$ is both an "exact" answer and an upper bound, all subject to the statistical errors. The improvement over the variational result is 2 MeV. There is no evidence of a rapid increase in statistical error as τ increases, indicating a more deeply bound state. At the moment Carlson is implementing the spin-orbit interaction in the GFMC procedure and plans to calculate with the RSC V_8 and Argonne V_3 potentials.

We argued previously that in general there was a lower energy eigenstate of the Hamiltonian which did not satisfy the Pauli principle. Why is such a state not seen? It is conventional to classify two-body states of a spin- and isospin-dependent Hamiltonian according to total spin (S) and isospin (T) for a given orbital state. Thus the generalized Pauli principle allows $S=1$ and $T=0$, as well as $S=0$ and $T=1$, for (antisymmetric) S-waves. If one relaxes that requirement, other combinations, such as $S=0$, $T=0$ and $S=1$, $T=1$, are allowed which would correspond to completely symmetric states under interchange of all coordinates. For a given angular momentum state (L and S) it is the isospin which implements the required change in symmetry. For example, the dominant tensor-coupled 3S_1 - 3D_1

partial waves become $T=1$. Moreover, the longest-range (and very important) force component arises from OPEP. The spin-isospin factor typical of the latter is $\vec{\sigma}_1 \cdot \vec{\sigma}_2 \vec{r}_1 \cdot \vec{r}_2$, which is -3 (attractive) for $(S,T) = (0,1)$ and $(1,0)$, but is repulsive for symmetric states. It is this feature of realistic nuclear forces which renders the s-wave components very repulsive for the symmetric states and consequently there is no bound symmetric state. This has been verified by a Faddeev calculation for such states [23], both with and without a three-nucleon force. The GFMC method offers great promise for the alpha particle where complete Faddeev-type calculations are exceptionally difficult.

The Faddeev method has been applied to a wide range of realistic potentials. These calculations are traditionally performed by expanding the nucleon-nucleon force into an infinite number of partial-wave potentials, each term of which acts only in a single partial wave (e.g., 1S_0). Calculations have been performed up to 34 channels (all NN waves with $J \leq 4$), although keeping more channels is quite possible. Variational calculations [26] for the additional components with $4 < J \leq 8$ indicate that only 10 keV is missing from the Faddeev calculations.

Results which have been obtained using 34-channels are: Reid Soft Core [27] (RSC) $[-7.36 \text{ MeV}]$; Argonne [25] V_{14} (AV14) $[-7.68 \text{ MeV}]$, Super Soft Core [28] (C) $[-7.53 \text{ MeV}]$, de Tourreil-Rouben-Sprung [29] (B) $[-7.57 \text{ MeV}]$, Paris [30] $[-7.64 \text{ MeV}]$ and Bonn [31] $[-8.33 \text{ MeV}]$ [32]. All are 34-channel results [33,34], and with the exception of the Bonn result [36,37] are roughly 1 MeV too low. See also Ref. [35] and [37]. The preliminary result from the LAFG for the Nijmegen potential is -7.77 MeV .

The Bonn potential has 3 significant features which presumably play some role in the increased binding. One feature of uncertain quantitative importance is the fact that the configuration space version of the most recent Bonn potential, like the Paris and Nijmegen potentials, has components of the form (\vec{p}^2, ϕ) , where \vec{p} is the relative two-body momentum. Such terms were neglected in almost all of the older semiphenomenological potentials, but they arise naturally [38] and are in fact required by special relativity [39]. The second feature is the weaker tensor force in the various Bonn potentials [31] (there are many such potentials with disparate forms and ages). It has been known for several decades that weakening the tensor force increases the triton binding energy. The reason is that although the triton binding is very sensitive to the tensor force, the deuteron is even more so. Consequently, the obvious requirement for any potential that the deuteron have the correct binding energy leads, upon weakening the tensor force, to a significantly enhanced central force, which is more effective in the triton than the deuteron and thus increases

the triton binding. Typical (but clearly unphysical) potential models without a tensor force overbind the triton.

The third feature which is salient is the fact that the potentials which are fitted solely to np scattering data are stronger than those fit also to pp data. The T=0 partial waves are determined solely by np data, but charge dependence of the force makes T=1 partial waves differ for the np and pp (or nn) cases; the s-wave scattering lengths prove this [38]. Consequently the 1S_0 potential for the AV14 and Bonn potentials, having been fit to np data, are stronger than those fit to pp data. Recently [40] we showed that if the tiny isoquartet (T=3/2) component of the trinucleon wave function produced by this charge dependence has a negligible effect, the appropriate T=1 NN force for use in the triton (assuming charge symmetry) is given simply by $(2V_{nn}/3 + V_{np}/3)$. Qualitatively this results from the 3 NN pairs in the triton being roughly 3/2 T=0 pairs and 3/2 T=1 pairs; there is one nn or pp pair (T=1), while each of the np pairs has a 3/4 T=0 (S=1) and 1/4 T=1 (S=0) weighting. Thus the force for the like particles (nn or pp) comes in with twice the weight of the unlike particles. The amount by which using V_{np} increases the binding over the "2/3-1/3 rule" given above is a model-dependent question, but simple estimates suggest that each "third" of a potential changes the binding energy by roughly 100 keV. Thus, using the 2/3-1/3 rule could reduce binding for np-fitted potentials by as much as .2 MeV and increase the binding for pp-fitted potentials by .1 MeV.

The weaker tensor force can presumably be put to an experimental test using NN data. Unfortunately, the relevant observables which are sensitive to the tensor force are poorly known, although there has been much recent experimental work which aims to improve the situation. Many of the details pertinent to constructing nucleon-nucleon potentials are decided by theoretical prejudice. Hopefully this question can be resolved soon.

Trinucleon Observables

Each of the methods we have described produces a wave function which can be used to calculate observables, such as the rms charge radii, asymptotic normalization constants, Coulomb energies, and charge densities. All of the methods which have been described calculate these observables routinely, as well as percentages of various wave function components, which are not measurable.

In addition to calculations based on two-nucleon potentials alone, there has been much recent activity in the area of three-nucleon forces. These forces add additional binding energy, in some cases a large amount. Consequently, there is a wide range of binding energies for these disparate

models. We will argue below that most of the trinucleon observables are sensitive to the trinucleon binding energy, E_B , and consequently, quoting a single number for such an observable has little meaning. What is a meaningful procedure in most circumstances is to plot the values of an observable for a particular model versus the corresponding binding energy of that model. Such plots are not new; the Phillips curve [41] for the nd doublet scattering length and the Tjon line [42] for the alpha particle binding are well-known examples. There is no guarantee that such a plot will show a distinct line, or narrow band. However, if such a dependence on E_B alone occurs, we say that "scaling" holds. This borrows from the vernacular of electromagnetic interactions, and means that E_B is the only effective variable which is required. The physical reasons for such a dependence are two-fold. If we restrict ourselves to "realistic" potentials, we guarantee that the long-range behavior of these forces is virtually identical. In addition, the triton is relatively diffuse like the deuteron ($E_B/A < 3$ MeV) and this tends to emphasize the regions of the wavefunction where the nucleons are noninteracting or scarcely interacting.

The paradigm for this behavior is the deuteron, whose asymptotic wave function is proportional to $\exp(-\kappa r)/r$, where $\kappa = E_B^{1/2}$. This form is completely determined by the binding energy, and illustrates why quoting observables without correlating them with the corresponding trinucleon binding energy is of limited value. In what follows below we show results for observables based only on LAFG calculations, not because others haven't performed similar calculations, but because these correlations can be easily made with our binding energies.

A good example of this scaling [43] is the rms charge radius. Schematic trinucleons are depicted below in Figure 2. The protons are shaded. If all NN forces were identical we would have the equilateral configuration in (2a). The rms charge radius is the (mean) distance (R_p) from the trinucleon center-of-mass (CM) to any one of the protons. Because the pp or nn force is weaker than the np force, the like particles actually lie further from the CM than the remaining unlike particle. Qualitatively, the angle θ in Figure (2b) is greater than 60° and the equilateral configuration (S-state) in (a) becomes isosceles in (b). The deviation of the isosceles from the equilateral configuration is a measure of the mixed symmetry S'-state. The geometry clearly indicates that the charge radius of ^3He is greater than that of ^3H . This is shown in Figure 3, a "scaling plot" of the rms charge radius, $\langle r^2 \rangle^{1/2}$, versus E_B for our theoretical data set. A point Coulomb interaction is included in the ^3He calculations [44]. The data from a Saclay [45] analysis are in good agreement with the simple fits.

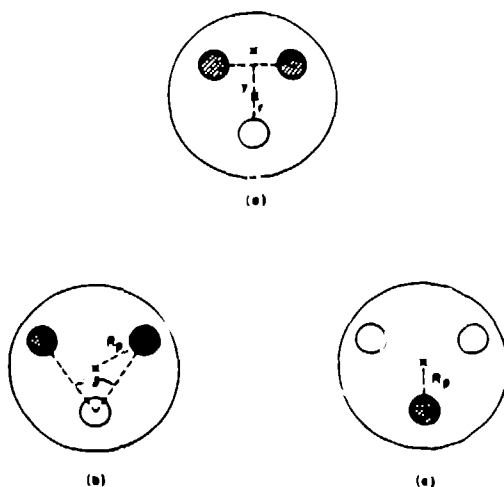


Figure 2. Schematic trinucleons with coordinates.

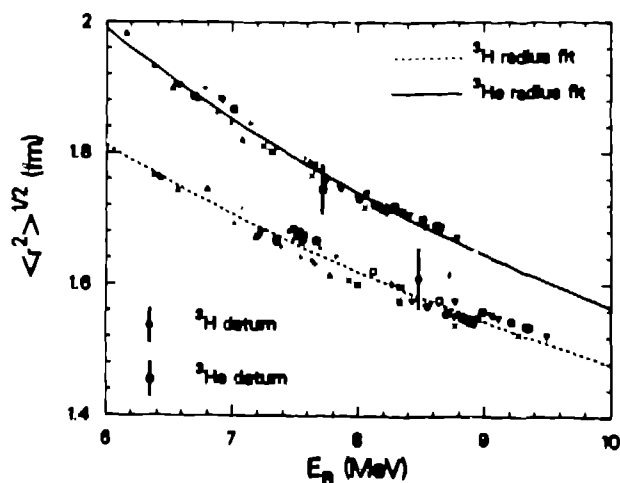


Figure 3. Scaling plot of rms charge radii calculations with fits and data.

The qualitative behavior can be easily understood. The mean-square radius is a matrix element which heavily weights the outer portion of the wavefunction, which schematically behaves as $\exp(-\kappa r)/r$, with $\kappa \sim (E_B)^{1/2}$. Assuming that the entire wavefunction has this form and performing the quadratures leads to $\langle r^2 \rangle^{1/2} \sim E_B^{-1/2}$. The isoscalar combination of rms radii $[(2\langle r^2 \rangle_{\text{He}} + \langle r^2 \rangle_{\text{H}})/3]^{1/2}$, does indeed vary in this fashion, while the difference component, which is largely determined by the S' -state, decreases more nearly as E_B^{-1} . The latter behavior can be traced to the rapid decrease of the probability of the S' -state, $P_{S'} \sim E_B^{-2}$, as a function of binding. This trend has a large spread and does not manifest scaling as

clearly as the rms radii [43]. Although not specifically included on our plot, the Bonn result [32] falls on the ^3H curve.

The pp Coulomb force produces two competing effects [44] on the ^3He charge radius. The Coulomb interaction lowers the binding energy and this increases the radius. In addition the asymptotic form of the wavefunction is changed from a Hankel function (exponential) to a Whittaker function, which falls more rapidly at large separations, thus reducing the radius.

The Coulomb energy of ^3He has long been known to be smaller than the 764 keV binding energy difference of ^3He and ^3H . The first quantitative demonstration of this was given by Fabre de la Ripelle [46] and Friar [47], who derived a simple approximation to the Coulomb energy which allowed experimental electron scattering data to be used to estimate that energy. The simplest version of that formula can be derived from Figure 2. The (point-nucleon) Coulomb potential in Figure (2a) is α/x , where α is the fine structure constant. If the trinucleons are primarily in an equilateral configuration, we can replace x by $\sqrt{3}r$, which in effect replaces the two-body correlation function by the charge density: $E_c = \langle \alpha/x \rangle = (\alpha/\sqrt{3}) \int d^3r \rho_{ch}(r)/r$. This simple approximation can be extended to include mixed-symmetry wave function components and the proton's charge distribution. It can be demonstrated [44] to work at the 1% level by calculating both sides of the relationship. If experimental data are used for ρ_{ch} one finds $E_c = 638 \pm 10$ keV. A scaling plot of E_c versus E_B , taking account of the proton's charge distribution, is shown in Figure 4. It produces $E_c = 652$ keV at $E_B = 8.48$ MeV. The slightly larger number results from the inability of theoretical wave functions to reproduce the inner portion of $\rho_{ch}(r)$, which leads to a small increase in E_c . The additional 100 keV which is needed is due to other direct and indirect charge-symmetry-breaking mechanisms.

Another important set of observables are the asymptotic normalization constants [32,48]. If one stretches the triton until a deuteron is outside the force range of the remaining neutron, the wave function becomes proportional to an exponential ($-\exp(-\beta y)$), where y is the relative coordinate of the two systems and β is the wave number for the deuteron-triton binding energy difference). The proportionality constant is the asymptotic normalization. Because of the NN tensor force, there are actually 2 constants, one for s-wave (C_S) and one for d-wave (C_D), and their ratio, $\eta = C_D/C_S$. There has been considerable recent interest in these constants for the analogous deuteron problem [49]. Because the wave number β increases as triton binding increases, the asymptotic wave function becomes steeper and probability decreases in the exterior region.

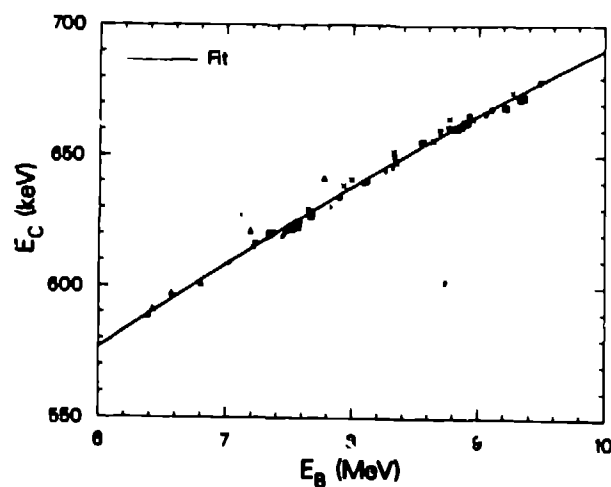


Figure 4. Scaling plot of ^3He Coulomb energy.

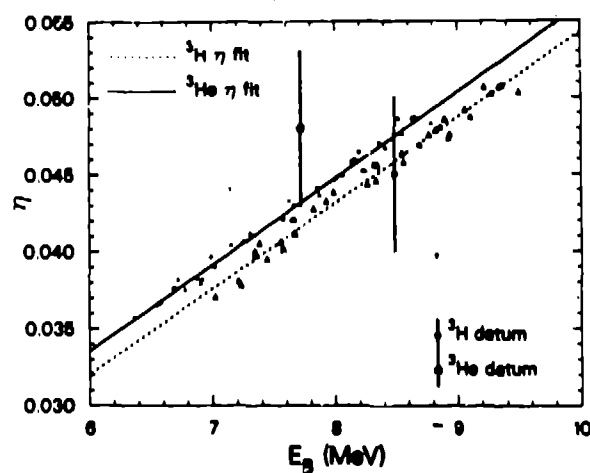


Figure 5. Scaling plot of asymptotic D/S ratio, with fits and data.

It becomes easier for the asymptotic wave function to match smoothly onto the interior portion if the asymptotic normalization constant increases as the binding increases. Each constant (C_S , C_D and η) increases with energy, as illustrated by η in Figure 5. Both ^3H and ^3He (with a Coulomb interaction) are shown together with data.

References

1. Y. Akaishi, *Few-Body Systems* (Suppl. 1), 120 (1986); *Lecture Notes in Physics* **273**, 324 (1987).
2. R. B. Wiringa, *Few-Body Systems* (Suppl. 1), 130 (1986).

3. C. Giofi degli Atti and S. Simula, Nuovo Cim. Lett. 41, 101 (1984).
4. K. E. Schmidt, Lecture Notes in Physics 273, 363 (1987).
5. J. L. Friar, B. F. Gibson, and G. L. Payne, Phys. Rev. C24, 2279 (1981).
6. M. H. Kalos, Phys. Rev. 128, 1791 (1962).
7. J. Carlson, LA-JR-87-1372, Los Alamos Preprint.
8. Yu. A. Simonov, Yad. Fiz. 3, 630 (1966).
9. M. Fabre de la Ripelle, Lecture Notes in Physics 273, 283 (1987).
10. B. A. Fomir and V. D. Efros, Yad. Fiz. 34, 587 (1981).
11. L. D. Faddeev, Zh. Eksp. Teor. Fiz. 39, 1459 (1960).
12. G. L. Payne, Lecture Notes in Physics 273, 64 (1987).
13. W. Glöckle, Lecture Notes in Physics 273, 3 (1987).
14. J. L. Friar, B. F. Gibson, and G. L. Payne, Ann. Rev. Nucl. Part. Sci. 34, 403 (1984).
15. R. A. Malfliet and J. A. Tjon, Nucl. Phys. A127, 161 (1969); Ann. Phys. (N.Y.) 61, 425 (1970).
16. J. Lomnitz-Adler, V. R. Pandharipande, and R. A. Smith, Nucl. Phys. A361, 399 (1981).
17. M. Fabre de la Ripelle [Private Communication]. This result is preliminary.
18. J. G. Zabolitzky, K. E. Schmidt, and M. H. Kalos, Phys. Rev. C25, 1111 (1982).
19. J. Carlson and V. R. Pandharipande, Nucl. Phys. A271, 301 (1981).
20. R. B. Wiringa [Private Communication].
21. J. L. Ballot and M. Fabre de la Ripelle, Ann. Phys. (N.Y.) 127, 62 (1980).
22. M. I. Mukhtarova [Private Communication].
23. J. Carlson, J. L. Friar, and G. L. Payne, LA-UR-87-2481, Los Alamos Preprint.
24. K. E. Schmidt and M. H. Kalos, Topics in Current Physics 36 (Springer, Berlin, 1984), p. 125.
25. R. B. Wiringa, R. A. Smith, and T. A. Ainsworth, Phys. Rev. C29, 1207 (1984).
26. J. L. Friar, B. F. Gibson, and G. L. Payne, LA-UR-87-1233, Los Alamos Preprint.
27. R. V. Reid, Ann. Phys. (N.Y.) 50, 411 (1968).
28. R. de Tourreil and D. W. L. Sprung, Nucl. Phys. A201, 193 (1973).
29. R. de Tourreil, B. Rouben, and D. W. L. Sprung, Nucl. Phys. A242, 445 (1975).
30. M. Lacombe, et al., Phys. Rev. C21, 861 (1980); *ibid.* D12, 1495 (1975).

31. R. Machleidt, K. Holinde, and C. Elster, Phys. Repts. 149, 1 (1987).
32. T. Sasakawa, Nucl. Phys. A463, 327c (1987).
33. C. R. Chen, G. L. Payne, J. L. Friar, and B. F. Gibson, Phys. Rev. C31, 2266 (1985); *ibid.* C33, 1740 (1986).
34. S. Ishikawa and T. Sasakawa, Few-Body Systems 1, 143 (1986); *ibid.* 1, 3 (1986).
35. C. Hajduk and P. U. Sauer, Nucl. Phys. A369, 321 (1981).
36. R. A. Brandenburg, et al., LA-UR-86-3700, Los Alamos Preprint.
37. J. Haidenbauer and Y. Koike, Phys. Rev. C34, 1187 (1986).
38. M. M. Nagels, T. A. Rijken and J. J. de Swart, Phys. Rev. D17, 768 (1978).
39. S. A. Coon and J. L. Friar, Phys. Rev. C34, 1060 (1986).
40. J. L. Friar, B. F. Gibson, and G. L. Payne, LA-UR-87-1153, Los Alamos Preprint.
41. A. C. Phillips, Rep. Prog. Phys. 40, 905 (1977).
42. J. A. Tjon, Phys. Lett. 56B, 217 (1975); Phys. Rev. Lett. 40, 1239 (1978).
43. J. L. Friar, B. F. Gibson, C. R. Chen, and G. L. Payne, Phys. Lett. 161B, 241 (1985).
44. J. L. Friar, B. F. Gibson, and G. L. Payne, Phys. Rev. C35, 1502 (1987).
45. F. P. Juster, et al., Phys. Rev. Lett. 55, 2261 (1985).
46. M. Fabre de la Ripelle, Fizika 4, 1 (1972).
47. J. L. Friar, Nucl. Phys. A156, 43 (1970).
48. J. L. Friar, B. F. Gibson, D. R. Lehman, and G. L. Payne, Phys. Rev. C25, 1616 (1982).
49. T. E. O. Ericson and M. Rosa-Clot, Ann. Rev. Nucl. Part. Sci. 35, 271 (1985).